

Phenomenology of Universal Extra Dimensions

Kyoungchul Kong¹ and Konstantin T. Matchev

Physics Department, University of Florida, Gainesville, FL 32611, USA

Abstract. In this proceeding, the phenomenology of Universal Extra Dimensions (UED), in which all the Standard Model fields propagate, is explored. We focus on models with one universal extra dimension, compactified on an S_1/Z_2 orbifold. We revisit calculations of Kaluza-Klein (KK) dark matter without an assumption of the KK mass degeneracy including all possible coannihilations. We then contrast the experimental signatures of low energy supersymmetry and UED.

Keywords: Dark Matter, Beyond Standard Model, Field Theories in Higher Dimensions

PACS: 11.10.Kk, 12.60.-i, 12.60.Jv, 14.80.Ly

INTRODUCTION

Models of UED place all Standard Model particles in the bulk of one or more compactified extra dimensions. In the simplest and most popular version, there is a single extra dimension of size R , compactified on an S_1/Z_2 orbifold [1]. A peculiar feature of UED is the conservation of Kaluza-Klein number at tree level, which is a simple consequence of momentum conservation along the extra dimension. However, bulk and brane radiative effects [2] break KK number down to a discrete conserved quantity, the so called KK parity, $(-1)^n$, where n is the KK level. KK parity ensures that the lightest KK partners (those at level one) are always pair-produced in collider experiments, just like in the R -parity conserving supersymmetry models. KK parity conservation also implies that the contributions to various low-energy observables only arise at loop level and are small. As a result, the limits on the scale R^{-1} of the extra dimension from precision electroweak data are rather weak, constraining R^{-1} to be larger than approximately 250 GeV. An attractive feature of UED models with KK parity is the presence of a stable massive particle which can be a cold dark matter candidate [3, 6, 7, 8].

KALUZA-KLEIN DARK MATTER

The first and only comprehensive calculation of the UED relic density to date was performed in [3]. The authors considered two cases of LKP: the KK hypercharge gauge boson B_1 and the KK neutrino ν_1 . The case of B_1 LKP is naturally obtained in Minimal UED (MUED) [9], where the radiative corrections to B_1 are the smallest in size, since they are only due to hypercharge interactions. The authors of [3] also realized the importance of coannihilation processes and included in their analysis coannihilations with the $SU(2)_W$ -singlet KK leptons, which in MUED are the lightest among the remaining $n = 1$

¹ current address: Theoretical Physics Department, Fermilab, Batavia, IL 60510, USA

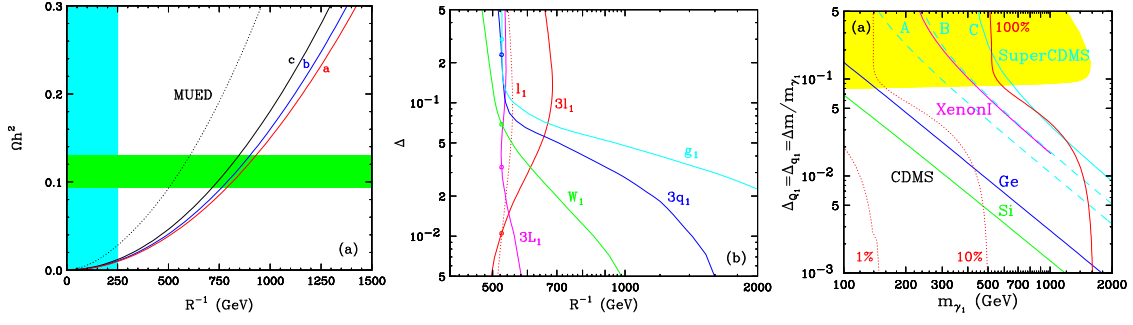


FIGURE 1. (a) Relic density of the LKP as a function of R^{-1} in the MUED model. (b) The change in the cosmologically preferred value for R^{-1} as a result of varying the different KK masses away from their nominal MUED values. (c) The spin-independent direct detection limit from CDMS experiment for γ_1

KK particles. It was therefore expected that their coannihilations will be most important. Subsequently, Ref. [4] analyzed the resonant enhancement of the $n = 1$ (co)annihilation cross-sections due to $n = 2$ KK particles and ref. [5] considered the influence of gravitons on the final relic density results. Here we complete the LKP relic density calculation of Ref. [3] and summarize our result. Fig. 1(a) shows the relic density of the LKP as a function of R^{-1} in the Minimal UED model. The (red) line marked “a” is the result from considering $\gamma_1 \gamma_1$ annihilation only, following the analysis of Ref. [3], assuming a degenerate KK mass spectrum. The (blue) line marked “b” repeats the same analysis, but uses T -dependent, effectively massless degrees of freedom and includes the relativistic correction to the b -term in the non-relativistic velocity expansion. The (black) line marked “c” relaxes the assumption of KK mass degeneracy, and uses the actual MUED mass spectrum. The dotted line is the result from the full calculation in MUED, including all coannihilation processes, with the proper choice of masses. The green horizontal band denotes the preferred WMAP region for the relic density $0.094 < \Omega_{CDM} h^2 < 0.129$. The cyan vertical band delineates values of R^{-1} disfavored by precision data.

Fig. 1(b) shows the change in the cosmologically preferred value for R^{-1} as a result of varying the different KK masses away from their nominal MUED values. Along each line, the LKP relic density is $\Omega_{\chi} h^2 = 0.1$. To draw the lines, we first fix the MUED spectrum, and then vary the corresponding KK mass and plot the value of R^{-1} which is required to give $\Omega_{\chi} h^2 = 0.1$. We show variations of the masses of one (red dotted) or three (red solid) generations of $SU(2)_W$ -singlet KK leptons; three generations of $SU(2)_W$ -doublet leptons (magenta); three generations of $SU(2)_W$ -singlet quarks (blue) (the result for three generations of $SU(2)_W$ -doublet quarks is almost identical); KK gluons (cyan) and electroweak KK gauge bosons (green). The circle on each line denotes the MUED values of Δ and R^{-1} .

The spin-independent direct detection limit from CDMS experiment is shown in fig. 1(c). We show the relic density and spin-independent direct detection limit from CDMS experiment in the plane of mass splitting $\Delta_{Q_1} = \Delta_{q_1} = \frac{m_{Q_1} - m_{\gamma_1}}{m_{\gamma_1}}$ and LKP mass for γ_1 LKP. The red line accounts for all of the dark matter (100%) and the two red dotted lines show 10% and 1%, respectively. The blue (green) line shows the current CDMS limit with Ge-detector (Si-detector) and the three cyan lines represent projected

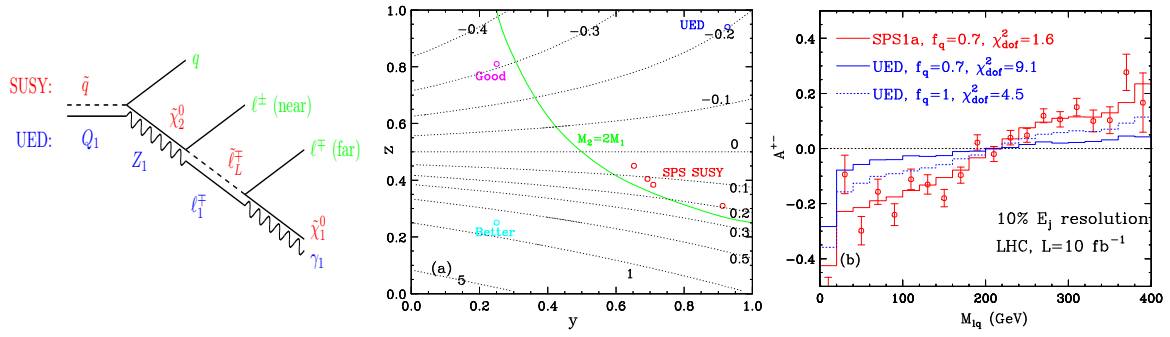


FIGURE 2. Spin determinations at the LHC using (a) the dilepton mass and (b) the asymmetry

SuperCDMS limits for each phase: A (25 kg), B (150 kg) and C (1 ton) respectively. In the case of γ_1 LKP, SuperCDMS rules out most of parameter space. The yellow region in the case of γ_1 LKP shows parameter space that could be covered by the collider search in $4\ell + E_T$ channel at the LHC [9].

DISCRIMINATION OF SUSY AND UED

We see that while R -parity conserving SUSY implies a missing energy signal, the reverse is not true: a missing energy signal would appear in any model with a dark matter candidate, and even in models which have nothing to do with the dark matter issue, but simply contain new neutral quasi-stable particles. Similarly, the equality of the couplings is a celebrated test of SUSY. It is only a necessary, but not a sufficient condition in proving supersymmetry. We are therefore forced to concentrate on discrimination between SUSY and UED. There are two fundamental distinctions between them. Let us begin with feature 1: the number of new particles. The KK particles at $n = 1$ are analogous to superpartners in supersymmetry [9]. The particles at the higher KK levels have no analogues in $N = 1$ supersymmetric models. Discovering the $n \geq 2$ levels of the KK tower would therefore indicate the presence of extra dimensions rather than SUSY. However these KK particles can be too heavy to be observed. Even if they can be observed at the LHC, they can be confused with other new particles [10, 11] such as Z' or different types of resonances from extra dimensions [12]. The discovery opportunities for the $n = 2$ level at the LHC and the Tevatron are discussed in [11] (for linear collider studies of $n = 2$ KK gauge bosons, see [10, 13]).

The second feature – the spins of the new particles – also provides a tool for discrimination between SUSY and UED. Recently it has been suggested that a charge asymmetry in the lepton-jet invariant mass distributions from a particular cascade, can be used to discriminate SUSY from the case of pure phase space decays [14] and is an indirect indication of the superparticle spins. It is therefore natural to ask whether this method can be extended to the case of SUSY versus UED discrimination [10, 11, 15]. Following [14], we concentrate on the cascade decay $\tilde{q} \rightarrow q \tilde{\chi}_2^0 \rightarrow q \ell^\pm \tilde{\ell}_L^\mp \rightarrow q \ell^\pm \ell^\mp \tilde{\chi}_1^0$ in SUSY and the analogous decay chain $Q_1 \rightarrow q Z_1 \rightarrow q \ell^\pm \tilde{\ell}_1^\mp \rightarrow q \ell^\pm \ell^\mp \gamma$ in UED (see fig. 2(a)). The invariant mass distributions for SUSY/Phase space can be written as $\frac{dN}{d\hat{m}} = 2\hat{m}$, while

for UED it is $\frac{dN}{d\hat{m}} = \frac{4(y+4z)}{(1+2z)(2+y)} (\hat{m} + r\hat{m}^3)$ [15?]. The coefficient r in the second term of the UED distribution is defined as $r = \frac{(2-y)(1-2z)}{y+4z}$, $\hat{m} = \frac{m_{\ell\ell}}{m_{\ell\ell}^{\max}}$ is the rescaled invariant mass, $y = \left(\frac{m_{\tilde{\ell}}}{m_{\tilde{\chi}_2^0}}\right)^2$ and $z = \left(\frac{m_{\tilde{\chi}_1^0}}{m_{\tilde{\ell}}}\right)^2$ are the ratios of the masses involved in the decay. y and z are less than 1 in the case of on-shell decay. We see that whether or not the UED distribution is the same as the SUSY distribution depends on the size of the coefficient r in the second term of the UED distribution. The UED distribution becomes exactly the same as the SUSY distribution if $r = 0.5$. Therefore we scan the (y, z) parameter space, calculate the coefficient r and show our result in fig. 2(a). In fig 2(a) contour dotted lines represent the size of the coefficient r . The minimal UED case is denoted by the blue dot in the upper-right corner since y and z are almost 1 due to the mass degeneracy. The red dots represent several snowmass points: SPS1a, SPS1b, SPS5 and SPS3 from left to right. The green line represents gaugino unification so all SUSY benchmark points are close to this green line. In fig. 2(b), we generated data samples from SPS1a assuming $10fb^{-1}$ and constructed the asymmetries in SUSY and UED. We included 10% jet energy resolution. Red dots represent data points, the red line is the SUSY fit to the data points and the blue lines are the UED fits to the data points for two different f_q 's. χ^2 -minimized UED (SUSY) fits to data are shown in blue (red). For SUSY, χ^2 is around 1 as we expect. We can get better χ^2 for UED from 9.1 to 4.5 by increasing f_q . It is still too big to fit the experimental data. So our conclusion for this study is that a particular point like SPS1a can not be faked through the entire parameter space of UED. However we need to check whether this conclusion will remain the same when we include the wrong jets which have nothing to do with this decay chain.

ACKNOWLEDGMENTS

The work of KK and KM is supported in part by a US Department of Energy Outstanding Junior Investigator award under grant DE-FG02-97ER41209.

REFERENCES

1. T. Appelquist, H. C. Cheng and B. A. Dobrescu, Phys. Rev. D **64**, 035002 (2001)
2. H. C. Cheng, K. T. Matchev and M. Schmaltz, Phys. Rev. D **66**, 036005 (2002)
3. G. Servant and T. M. Tait, Nucl. Phys. B **650**, 391 (2003)
4. M. Kakizaki, S. Matsumoto, Y. Sato and M. Senami, arXiv:hep-ph/0508283.
5. N. R. Shah and C. E. M. Wagner, arXiv:hep-ph/0608140.
6. F. Burnell and G. D. Kribs, Phys. Rev. D **73**, 015001 (2006)
7. K. Kong and K. T. Matchev, JHEP **0601**, 038 (2006)
8. H. C. Cheng, J. L. Feng and K. T. Matchev, Phys. Rev. Lett. **89**, 211301 (2002)
9. H. C. Cheng, K. T. Matchev and M. Schmaltz, Phys. Rev. D **66**, 056006 (2002)
10. M. Battaglia, A. K. Datta, A. De Roeck, K. Kong and K. T. Matchev, arXiv:hep-ph/0507284.
11. A. Datta, K. Kong and K. T. Matchev, Phys. Rev. D **72**, 096006 (2005)
12. G. Burdman, B. A. Dobrescu and E. Ponton, arXiv:hep-ph/0601186.
13. M. Battaglia, A. Datta, A. De Roeck, K. Kong and K. T. Matchev, JHEP **0507**, 033 (2005)
14. A. J. Barr, Phys. Lett. B **596**, 205 (2004)
15. J. M. Smillie and B. R. Webber, JHEP **0510**, 069 (2005)